

U(1)' coupling constant at low energies from heterotic orbifolds

Yessenia Olguín-Trejo,^{1*} Omar Pérez-Figueroa,^{1†} Ricardo Pérez-Martínez^{1,2‡}
and Saúl Ramos-Sánchez^{1§}

¹*Instituto de Física, Universidad Nacional Autónoma de México,
POB 20-364, Cd.Mx. 01000, México*

²*Facultad de Ciencias Físico-Matemáticas, Universidad Autónoma de Coahuila,
Edificio A, Unidad Camporredondo, 25000, Saltillo, Coahuila, México*

Abstract

Additional Abelian gauge interactions are generic to string compactifications. In heterotic string models, gauge coupling unification of such forces and other gauge interactions is natural due to their common origin. In this letter we study systematically the 1-loop running of the coupling constants in effective vacua emerging from \mathbb{Z}_8 heterotic orbifold compactifications that provide the matter spectrum of the MSSM plus some vectorlike exotics, restricting to vacua that yield a non-anomalous U(1)' symmetry, gauge coupling unification and the observed values of known gauge couplings. We determine the low-energy value of the U(1)' coupling constant for different scales of supersymmetry breakdown. We find that the U(1)' coupling constant is quite restricted in string models to lie in the range 0.46–0.7 for low-scale supersymmetry or 0.44–0.6 in other cases. We argue that the phenomenology of these string vacua should be further explored to solve some extant issues, such as the stability of the Higgs vacuum.

*yes.olt@ciencias.unam.mx

†omar_perfig@ciencias.unam.mx

‡ricardoperez@estudiantes.fisica.unam.mx

§ramos@fisica.unam.mx

1 Introduction

Some open questions in the standard model (SM) and cosmology have led to conjecture the existence of additional $U(1)'$ gauge symmetries, under which different SM particles may be charged. These symmetries lead to a rich phenomenology (for details, see ref. [1] and references therein). To mention a few of their qualities, they may shed some light on neutrino physics and dark matter simultaneously [2–4], or the $g_\mu - 2$ anomaly [5], or the metastability of the Higgs vacuum [6]. They could also yield interesting signals at colliders [7–9] and alleviate some issues of models with supersymmetry (SUSY) [10, 11]. Although they must be broken at low energies and $m_{Z'}$ is very constrained [12–15], the bounds can be avoided (e.g. via a leptophobic $U(1)'$) and Z' signals could be soon confirmed at colliders.

The origin of $U(1)'$ symmetries is frequently related to grand unified theories (GUT) beyond $SU(5)$. For example, in E_6 GUTs, $U(1)'$ symmetries have been classified and studied phenomenologically [16–19]. It is also known that $U(1)$'s are natural to models resulting from different string compactifications [20–23]. In particular, in heterotic orbifolds in the fermionic formulation, plausible scenarios with a light Z' and rich phenomenology have been identified [22, 24, 25]. Also, orbifolds in the bosonic formulation have shown that in models resembling the minimal extension of the SM (the MSSM), matter parity [26, 27] or even a \mathbb{Z}_4^R symmetry [28] for proton stability can arise from $U(1)$'s (and other symmetries) of the model.

Motivated by these findings, in this letter we aim at characterizing the couplings of non-anomalous $U(1)$'s natural to some string compactifications. We focus on \mathbb{Z}_8 toroidal orbifold compactifications of the $E_8 \times E_8$ heterotic string with MSSM-like features. This kind of models has been investigated before [29], but with a different purpose and only in a small subset (about 20%) of all promising models due to some far too restrictive priors which do not improve the phenomenology of the models. We avoid such restrictions to obtain a richer variety of models and a more general analysis.

We study special *effective vacua* with gauge group $SU(3)_c \times SU(2)_L \times U(1)_Y \times U(1)'$, where the kinetic mixing of Abelian symmetries is unimportant [30] and the few exotics in their spectra are vectorlike w.r.t. the SM. Assuming that a Higgs-like mechanism breaks the $U(1)'$ at a scale $\Lambda_{Z'} = 2$ TeV, where also some exotics acquire masses, and a SUSY breaking scale $\Lambda_{SUSY} \geq \Lambda_{Z'}$, we determine systematically the running of all coupling constants of our effective vacua by using the renormalization group equations (RGE) at 1-loop, which suffice at this level because of further small corrections that we neglect, such as threshold effects. Restricting to vacua with gauge coupling unification, we observe that besides the usual family non-universality of stringy $U(1)$'s, heterotic orbifolds limit the values of the $U(1)'$ coupling at the TeV scale as well as the unification scale and the unified coupling.

In what follows, we discuss the main features of \mathbb{Z}_8 heterotic orbifold compactifications and their effective vacua with $U(1)'$ and analyze how to arrive at limits for the couplings of such symmetries. Our findings are reported in section 4, followed by a sample model with the potential to solve the metastability of the Higgs vacuum thanks to a $U(1)'$.

2 MSSM-like \mathbb{Z}_8 toroidal orbifold models

Our starting point is the $\mathcal{N} = 1$ $E_8 \times E_8$ heterotic string theory in the bosonic formulation, and we compactify the six extra dimensions on a toroidal \mathbb{Z}_8 orbifold that preserves $\mathcal{N} = 1$ in four dimensions. This choice is taken because \mathbb{Z}_8 has shown to be the symmetry that yields the largest fraction of \mathbb{Z}_N MSSM-like heterotic orbifold models available so far [31], so that we can be sure to be focused on a representative patch of promising string compactifications.

In general, a toroidal \mathbb{Z}_N orbifold is defined as the quotient \mathbb{T}^6/P of a six-torus over a point group, which is generated by a single twist ϑ of order N , i.e. so that $\vartheta^N = \mathbb{1}$. ϑ must be chosen to act as an isometry on \mathbb{T}^6 . ϑ can always be diagonalized on three two-dimensional actions, so that $\vartheta = \text{diag}(e^{2\pi i v_1}, e^{2\pi i v_2}, e^{2\pi i v_3})$, where $v = (v_1, v_2, v_3)$ is called the *twist vector*. It is possible to combine together the point group with the lattice Γ of the torus to build the space group $S = P \ltimes \Gamma$, such that the orbifold can be analogously defined as \mathbb{R}^6/S .

A complete classification of the \mathbb{T}^6 geometries and point groups for Abelian toroidal orbifolds [32] reveals that there are only two \mathbb{Z}_8 point groups, denoted $\mathbb{Z}_8\text{-I}$ and $\mathbb{Z}_8\text{-II}$ and defined by the twist vectors $v_{\mathbb{Z}_8\text{-I}} = \frac{1}{8}(1, 2, -3)$ and $v_{\mathbb{Z}_8\text{-II}} = \frac{1}{8}(1, 3, -4)$, respectively. There are five inequivalent \mathbb{T}^6 geometries (see [29] for details) acceptable for these twists. Following the notation of [32], we shall label them as $\mathbb{Z}_8\text{-I} (i, 1)$, $i = 1, 2, 3$, and $\mathbb{Z}_8\text{-II} (j, 1)$, $j = 1, 2$.

A consistent heterotic orbifold requires to embed the action of the six-dimensional orbifold into the $E_8 \times E_8$ gauge degrees of freedom. The \mathbb{Z}_N twist ϑ can be embedded as a 16-dimensional *shift vector* V of order N (i.e. such that NV is in the $E_8 \times E_8$ root lattice), whereas the six independent directions of the torus can be embedded as 16-dimensional discrete *Wilson lines* (WL) W_a , $a = 1, \dots, 6$. Given a \mathbb{Z}_N twist and a toroidal geometry, there are several admissible choices of shifts and WL, as long as they fulfill the *modular invariance conditions* [33],

$$\begin{aligned} N(V^2 - v^2) &= 0 \pmod{2}, & N_a(V \cdot W_a) &= 0 \pmod{2}, & a &= 1, \dots, 6, \\ N_a W_a^2 &= 0 \pmod{2}, & \gcd(N_a, N_b)(W_a \cdot W_b) &= 0 \pmod{2}, & a &\neq b, \end{aligned} \quad (1)$$

which ensure that the four-dimensional emergent field theory be non-anomalous and compatible with string theory. The space group of the orbifold constrains the order¹ N_a of a WL W_a and its relations with other WL. Interestingly, these restrictions can be understood in terms of the Abelianization of the space group as requirements for the WL to be compatible with the embedding of the so-called space group flavor symmetry into the gauge degrees of freedom [34].

In \mathbb{Z}_8 orbifolds, the order and relations of the admissible WL are given in table 1. Two $\mathbb{Z}_8\text{-I}$ geometries admit two independent WL of order two, whereas the third case admits only one independent order-4 WL. Further, $\mathbb{Z}_8\text{-II} (1, 1)$ allows for three order-2 WL, and $\mathbb{Z}_8\text{-II} (2, 1)$, one WL of order two and one of order four.

Applying standard techniques (see e.g. [35–38]), one can use the modular invariant solutions to eqs. (1) (with $N = 8$) complying with the WL-constraints of table 1 to com-

¹The smallest integer N_a , such that $N_a W_a$ (with no summation over a) is contained in the root lattice of $E_8 \times E_8$, is defined as the *order of the WL* W_a .

Orbifold	Conditions on the Wilson lines
$\mathbb{Z}_8\text{-I} (1,1)$	$2W_1 \approx 2W_5 \approx 0; W_1 \approx W_2 \approx W_3 \approx W_4; W_5 \approx W_6$
$\mathbb{Z}_8\text{-I} (2,1)$	$2W_1 \approx 2W_5 \approx 0; W_1 \approx W_2 \approx W_3 \approx W_4; W_5 \approx W_6$
$\mathbb{Z}_8\text{-I} (3,1)$	$4W_1 \approx 0; W_1 \approx W_2 \approx W_3 \approx W_4 \approx W_5 \approx W_6$
$\mathbb{Z}_8\text{-II} (1,1)$	$2W_1 \approx 2W_5 \approx 2W_6 \approx 0; W_1 \approx W_2 \approx W_3 \approx W_4$
$\mathbb{Z}_8\text{-II} (2,1)$	$4W_1 \approx 2W_6 \approx 0; W_1 \approx W_2 \approx W_3 \approx W_4 \approx W_5$

Table 1: Orders and relations of the WL of \mathbb{Z}_8 orbifolds, depending on the geometry of the compactification. $A \approx B$ indicates that $A = B$ up to translations in the root lattice of $E_8 \times E_8$.

pute the spectrum of massless string states. These techniques have been implemented in the `orbifolder` [39] to automatize the search of admissible models, the computation of the massless spectrum, and the identification of phenomenologically viable models. By using this tool, we have previously [31] found 3,431 \mathbb{Z}_8 orbifold compactifications of the $E_8 \times E_8$ heterotic string with the following properties:

- the gauge group at the compactification scale is

$$\mathcal{G}_{4D} = \mathcal{G}_{SM} \times [\mathrm{U}(1)']^n \times \mathcal{G}_{\text{hidden}}, \quad (2)$$

where $\mathcal{G}_{SM} = \mathrm{SU}(3)_c \times \mathrm{SU}(2)_L \times \mathrm{U}(1)_Y$ with non-anomalous hypercharge (satisfying $\sin^2 \theta_w = 3/8$), $\mathcal{G}_{\text{hidden}}$ is a non-Abelian gauge factor (typically a product of $\mathrm{SU}(M)$ subgroups), at most one $\mathrm{U}(1)'$ is (pseudo-)anomalous and $n \leq 10$, depending on the model; and

- the massless spectrum includes the MSSM superfields plus only vectorlike exotic matter w.r.t. \mathcal{G}_{SM} .

$\mathcal{G}_{\text{hidden}}$ is commonly considered a *hidden gauge group* because the MSSM fields are mostly uncharged under that group. The number of models found in each orbifold geometry is presented in table 2. The defining shifts and WL of the models can be found in [40].

Aiming at the study of the $\mathrm{U}(1)'$ symmetries of these models, we must point out some of their properties. Most of the models present an anomalous $\mathrm{U}(1)'$ [41], whose anomaly can be canceled through the Green-Schwarz mechanism [42]. Besides, in this type of models, the gauge fields of the $\mathrm{U}(1)'_\alpha$ symmetries can be decomposed as

$$T_\alpha = \sum_{I=1}^{16} t_\alpha^I H_I, \quad \alpha = 1, \dots, n, \quad (3)$$

in terms of the Cartan generators H_I of the original $E_8 \times E_8$, such that the corresponding $\mathrm{U}(1)'_\alpha$ charges for fields of the spectrum with gauge momentum $p \in E_8 \times E_8$ are given by $q_\alpha = t_\alpha \cdot p$. This is why t_α is frequently called the generator of $\mathrm{U}(1)'_\alpha$. It is known that, if we adopt² the $\mathrm{U}(1)'$ normalization $k|t_\alpha|^2 = 1$ and consider all algebras associated with the gauge group to have Kač-Moody level $k = 2$, the tree-level gauge kinetic function is universally given by

²Despite this $\mathrm{U}(1)'$ normalization, we allow the GUT-compatible hypercharge normalization $|t_1|^2 = 5/6$.

Orbifold	# MSSM-like models	effective vacua	Orbifold	# MSSM-like models	effective vacua
$\mathbb{Z}_8\text{-I}(1, 1)$	268	1,362	$\mathbb{Z}_8\text{-II}(1, 1)$	2,023	10,023
$\mathbb{Z}_8\text{-I}(2, 1)$	246	1,097	$\mathbb{Z}_8\text{-II}(2, 1)$	505	2,813
$\mathbb{Z}_8\text{-I}(3, 1)$	389	1,989			

Table 2: Number of inequivalent heterotic orbifold models with MSSM-like properties found in ref. [31] for each \mathbb{Z}_8 orbifold geometry. We further provide in the third and sixth columns the number of vacuum configurations with MSSM-like properties and gauge group $\mathcal{G}_{\text{eff}} = \mathcal{G}_{SM} \times \text{U}(1)'$ in each case.

$f_\alpha = S$, where S corresponds to the bosonic component of the (axio-)dilaton. Consequently, the tree-level gauge coupling satisfies $g_s^{-2} = \langle \text{Re}S \rangle$ at the (heterotic) string scale, $M_{str} \approx 10^{17}$ GeV. Further, there is some kinetic mixing between different $\text{U}(1)'$ gauge symmetries which one might believe relevant for phenomenology; however, it has been found to be typically of order 10^{-4} – 10^{-2} in semi-realistic heterotic orbifolds [30], unimportant for our purposes.

Let us make a couple of additional remarks about the models we explore. First, as in the MiniLandscape [27, 43, 44] of $\mathbb{Z}_6\text{-II}$ heterotic orbifolds, in all the \mathbb{Z}_8 models discussed here, there exists a large number of SM-singlets, which naturally develop $\mathcal{O}(0.1)$ VEVs in order to cancel the Fayet-Iliopoulos term, $\xi = g_s^2 \text{tr } T_{\text{anom}}/192\pi^2$ (in Planck units), appearing in models with a (pseudo-)anomalous $\text{U}(1)'$. As a consequence, the allowed couplings of such singlets among themselves and with vectorlike exotics yield large masses for the additional matter, decoupling it from the low-energy effective field theory. Simultaneously, since the singlets are charged under the $[\text{U}(1)']^n$ gauge sector, those symmetries can be broken in the vacuum.

Secondly, it is always possible to find SM-singlet VEV configurations, such that, SUSY is retained while only the *effective gauge group*,

$$\mathcal{G}_{\text{eff}} = \mathcal{G}_{SM} \times \text{U}(1)' \subset \mathcal{G}_{4D}, \quad (4)$$

remains after the spontaneous breakdown triggered by the singlet VEVs, where we ignore the hidden group $\mathcal{G}_{\text{hidden}}$. The surviving (non-anomalous) $\text{U}(1)'$ can be any of the original $\text{U}(1)'_\alpha$, $\alpha = 1, \dots, n$, symmetries or a linear combination of them, depending on the details of the model. In this work, for practical purposes, we shall study only the former case, i.e. the effective vacua with the effective gauge group \mathcal{G}_{eff} , where the $\text{U}(1)'$ corresponds to each of the non-anomalous $\text{U}(1)'_\alpha$ of the \mathbb{Z}_8 orbifold models. We find that there is a total of 17,284 such effective vacua, distributed in all admissible \mathbb{Z}_8 orbifold geometries, as shown in table 2.

Third, in the most general case, (at least) some of the MSSM superfields and the exotics exhibit some $\text{U}(1)'$ charges. This is true in most of the vacua where one of the $\text{U}(1)'$ remains unbroken. Thus, only the exotics that are vectorlike w.r.t. \mathcal{G}_{eff} , and not just \mathcal{G}_{SM} , decouple at low energies, allowing interactions among SM fields charged under $\text{U}(1)'$ and the extra matter which can yield interesting new phenomenology. These interactions affect in particular the RGE running of the gauge couplings, as we discuss in the following section.

3 Searching effective vacua with $U(1)'$ and unification

We shall study the value of the $U(1)'$ coupling constants of the effective field theories emerging from \mathbb{Z}_8 heterotic orbifold compactifications at currently reachable energies, restricting ourselves to those that are consistent with unification, in the sense that the gauge couplings meet (perhaps accidentally) at a given scale, and where SM gauge couplings are compatible with the observed values at low energies.

Selecting the vacua with these features requires some additional knowledge of the details of the effective spectrum, and some reasonable priors. The first hurdle is that, even though $g_s^{-2} = \langle \text{Re}S \rangle$ at M_{str} , below this scale, the coupling constants get different contributions from all other moduli too, whose stabilization represents a challenge by itself [45, 46], hindering to know the exact values of the gauge couplings in the effective field theory. Thus, in order to figure out which models yield the measured values of the gauge couplings, one could start with an *ad hoc* value of all SM gauge couplings at high energies and retain only models where the RGE lead to the observed values at M_Z . This approach seems rather arbitrary.

Instead, we assume that the SM coupling strengths α_i of our effective vacua have the observed values at M_Z [47], (with $i = 1$ for $U(1)_Y$, $i = 2$ for $SU(2)_L$ and $i = 3$ for $SU(3)_c$)

$$\alpha_1^{-1}(M_Z) = 59.01 \pm 0.01, \quad \alpha_2^{-1}(M_Z) = 29.59 \pm 0.01, \quad \alpha_3(M_Z) = 0.1182 \pm 0.0012, \quad (5)$$

and then let the RGE define the value of the gauge couplings at all scales up to M_{str} , using the spectrum of the effective vacua we find. These effective vacua exhibit $\mathcal{N} = 1$ SUSY and an additional Z' boson, but no SUSY partner (in some models, the lightest neutralino with masses lighter than few hundred GeV has been excluded [48, 49]) nor extra vector boson has been detected at the LHC so far (with a lower limit for $m_{Z'}$ around 2 TeV [12–15]). Hence, we suppose that SUSY is broken at a scale $\Lambda_{SUSY} > M_Z$ and the $U(1)'$ breakdown scale is $\Lambda_{Z'} = 2$ TeV, as a benchmark value.³ We further assume that $\Lambda_{SUSY} \geq \Lambda_{Z'}$.

Given these remarks, we consider different matter spectra depending on the energy scale μ . As sketched in figure 1, above the SUSY scale Λ_{SUSY} the spectrum of the effective vacua includes the MSSM superfields and a few vectorlike exotics w.r.t. \mathcal{G}_{SM} with non-trivial $U(1)'$ charges. Below Λ_{SUSY} , if it is larger than $\Lambda_{Z'}$, the gauge group is still \mathcal{G}_{eff} , eq. (4), but we assume that all SM superpartners and the bosonic superpartners of the exotics decouple. Only one SM singlet with $U(1)'$ charge is taken as scalar below Λ_{SUSY} , so that its VEV can trigger the breakdown of $U(1)'$ and provide masses around $\Lambda_{Z'}$ for the remaining exotics. Consequently, below $\Lambda_{Z'}$ only the SM particles and gauge group are left.

The next step is to choose only models that are consistent with gauge coupling unification, so that we recover at some level the unification provided at M_{str} by string theory, and justify why we have restricted ourselves to hypercharges with GUT normalization. To do so, we let the RGE determine the value of the SM couplings and retain vacua with unification at some

³We have verified that our results are qualitatively the same for other scales near this value.

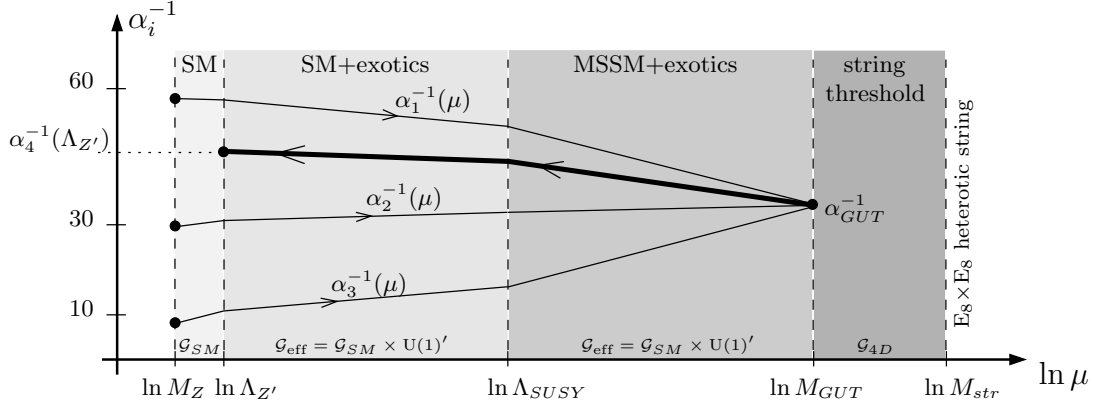


Figure 1: Our approach to determine the value at low energies of the $U(1)'$ coupling strength α_4 , the unification scale M_{GUT} and the unification value of the gauge couplings α_{GUT} . We consider $\Lambda_{Z'} = 2$ TeV, the three cases $\Lambda_{SUSY} = \Lambda_{Z'}, 10^{12}$ GeV, 10^{17} GeV and $M_{str} \approx 10^{17}$ GeV. We illustrate the case $\Lambda_{Z'} < \Lambda_{SUSY} < M_{GUT}$.

scale M_{GUT} , which varies from vacuum to vacuum due to their matter content.⁴ At M_{GUT} , one naturally can assume that all coupling strengths of \mathcal{G}_{eff} have the same value α_{GUT} . Thus, the $U(1)'$ coupling strength $\alpha_4 = \alpha_{GUT}$ at that scale and its RGE running down to $\Lambda_{Z'}$ in a vacuum is a low-energy consequence of such a vacuum. This approach is depicted in figure 1. We display an intermediate Λ_{SUSY} , but, in this work, we consider three well-motivated cases: $\Lambda_{SUSY} = \Lambda_{Z'}$, $\Lambda_{SUSY} = 10^{12}$ GeV and $\Lambda_{SUSY} = 10^{17}$ GeV. The first one arises from the common expectation that SUSY may show up at reachable energies, the second one from constraints on the metastability of the Higgs potential [50] and the last one from considering that SUSY may be broken at the string scale, as in non-SUSY string compactifications [51–53]. It is known that gaugino condensates can render various Λ_{SUSY} in these models [54].

As stated before, all vectorlike exotics w.r.t. \mathcal{G}_{eff} naturally acquire masses just below M_{str} while \mathcal{G}_{4D} breaks down to \mathcal{G}_{eff} , but it is easy to conceive that this process happens gradually at various scales between M_{GUT} and M_{str} . Furthermore, we expect that at those scales string threshold corrections, effects of the Green-Schwarz mechanism and moduli stabilization take place. We shall assume that all these effects do not alter the unification, even though they set deviations of α_{GUT} from $\alpha_s = g_s^2/4\pi$ that differ for each effective vacuum.

In this work, we use the 1-loop RGE for the gauge factors of the effective gauge group, $G_i \in \mathcal{G}_{eff}$. The running of the coupling strengths $\alpha_i = g_i^2/4\pi$ is given by

$$\frac{\partial \alpha_i^{-1}}{\partial \ln \mu} = -\frac{b_i}{2\pi}, \quad i = 1, \dots, 4, \quad (6)$$

⁴Note that, even though M_{GUT} defines the scale at which all gauge couplings meet, no true unification is implied in the sense of usual GUTs.

where the β -function coefficients for non-Abelian groups ($i = 2, 3$) are given at 1-loop by

$$b_i = \begin{cases} -\frac{11}{3}C_2(G_i) + \frac{2}{3}\sum_f m_f C(\mathbf{R}_f) + \frac{1}{3}\sum_b m_b C(\mathbf{R}_b), & \text{non-SUSY}, \\ -3C_2(G_i) + \sum_S m_S C(\mathbf{R}_S), & \text{SUSY}, \end{cases} \quad (7)$$

Here $C_2(G_i)$ is the quadratic Casimir of the group G_i , $C(\mathbf{R}_{b,f,S})$ denotes respectively the quadratic index of the G_i representations $\mathbf{R}_{b,f,S}$ of the bosons, fermions and superfields included in the spectrum, over which the sums run, and $m_{b,f,S}$ denotes their multiplicities. Conventionally, we take $C(\mathbf{R}_{b,f,S}) = 1/2$ if $\mathbf{R}_{b,f,S}$ corresponds to the fundamental representation of $SU(N)$. For Abelian gauge symmetries ($i = 1, 4$), eq. (7) reduces to

$$b_i = \begin{cases} \frac{2}{3}\sum_f m_f |q_i^{(f)}|^2 + \frac{1}{3}\sum_b m_b |q_i^{(b)}|^2, & \text{non-SUSY}, \\ \sum_S m_S \text{tr} |q_i^{(S)}|^2, & \text{SUSY}. \end{cases} \quad (8)$$

in terms of the matter $U(1)'$ charges $q_i^{(b,f,S)}$, defined around eq. (3).

The solutions to (6) have the general form $\alpha_i^{-1}(\mu) = \alpha_i^{-1}(\mu_0) - b_i/2\pi \ln(\mu/\mu_0)$, in terms of a reference scale μ_0 . For the SM couplings, we take their observed values, eq. (5), with $\mu_0 = M_Z$. Since below $\Lambda_{Z'} = 2$ TeV we assume that only the SM particles are present, we determine readily that $\alpha_1^{-1} = 56.99$, $\alpha_2^{-1} = 31.15$ and $\alpha_3^{-1} = 11.9$ at $\Lambda_{Z'}$.

4 $U(1)'$ couplings in \mathbb{Z}_8 heterotic orbifold vacua

As a first step, we compute systematically the β -function coefficients, according to eqs. (7)-(8), of all effective vacua counted in table 2. We observe that a fraction (3.5%) of all vacua yield the properties of the MSSM above Λ_{SUSY} . That is, their matter spectra match the MSSM spectrum and, consequently, $(b_1, b_2, b_3, b_4) = (33/5, 1, -3, 0)$. In these cases, $b_4 = 0$ arises because the MSSM fields have no $U(1)'$ charges. In the second column of table 3 we show the number of these MSSM vacua. There is also a smaller fraction (1.3%) of vacua with $b_4 = 0$, but $b_i \neq b_i^{MSSM}$. Since in all these cases the coupling of Z' with observable matter is very suppressed, we shall not consider these models here.

The running of the couplings described by the RGE reveals that there is a significant number of vacua that are inadmissible for our study. First, computing the scale at which couplings meet leads in some cases to $M_{GUT} < M_Z$ or $M_{GUT} > M_{str}$, which are either excluded (the former) or meaningless since our effective models apply only below M_{str} . Second, vacua in which any of the coupling strengths $\alpha_i = g_i^2/4\pi$ reaches negative values in its running are not acceptable. Finally, since our work is based on weakly coupled string theory, non-perturbative couplings, $\alpha_i > 1$, are equally undesirable.

The number of vacua with these weaknesses varies depending on the choice of Λ_{SUSY} and the \mathbb{Z}_8 orbifold geometry. For instance, in the case of \mathbb{Z}_8 -I (1,1) with $\Lambda_{SUSY} = \Lambda_{Z'} = 2$ TeV, we find that out of the 1,362 effective vacua, 205 lead to unification at a scale $M_{GUT} < \Lambda_{Z'}$ or $M_{GUT} > M_{str}$. Further, 321 vacua produce negative values of some α_i , and in 89 we find non-

orbifold	MSSM vacua	effective vacua of interest					
		$\Lambda_{SUSY} = \Lambda_{Z'}$		$\Lambda_{SUSY} = 10^{12} \text{ GeV}$		$\Lambda_{SUSY} = 10^{17} \text{ GeV}$	
		$\alpha_1 = \alpha_2$	unified	$\alpha_1 = \alpha_2$	unified	$\alpha_1 = \alpha_2$	unified
$\mathbb{Z}_8\text{-I (1,1)}$	58	681	2	1,218	8	1,253	20
$\mathbb{Z}_8\text{-I (2,1)}$	116	421	0	940	2	958	3
$\mathbb{Z}_8\text{-I (3,1)}$	76	1,101	8	1,792	7	1,844	20
$\mathbb{Z}_8\text{-II (1,1)}$	245	6,476	60	8,970	181	9,245	114
$\mathbb{Z}_8\text{-II (2,1)}$	111	1,929	7	2,567	71	2,631	51
totals	606	10,608	77	15,487	269	15,931	208

Table 3: Number of effective MSSM-like vacua arising from \mathbb{Z}_8 heterotic orbifolds with $U(1)'$ symmetries and gauge coupling unification. For each orbifold geometry, the second column shows the number of vacua with the exact dynamics of the MSSM, i.e. such that $b_i = b_i^{MSSM} \in \{33/5, 1, -3, 0\}$ in their RGE. Excluding these and other inconsistent models, in the remaining (pairs of) columns we show the number of vacua satisfying our constraints and with partial unification ($\alpha_1 = \alpha_2$) or total gauge coupling unification ($\alpha_{GUT} = \alpha_i$), corresponding to three choices of Λ_{SUSY} .

perturbative values for some couplings ($\alpha_i > 1$). Disregarding these (and those with $b_4 = 0$), we arrive at the 681 vacua of table 2 for this case.

To obtain the \mathbb{Z}_8 orbifold vacua of interest, with unification of all coupling strengths, we proceed in two steps. We analyze first the qualities of those vacua with $SU(2)_L - U(1)_Y$ unification, i.e. those with $\alpha_1 = \alpha_2 \neq \alpha_3$, and then select among them those with $\alpha_{GUT} \equiv \alpha_1 = \alpha_2 \approx \alpha_3$ at a scale M_{GUT} , allowing for a small deviation $|\alpha_{GUT}^{-1} - \alpha_3^{-1}(M_{GUT})| < 0.26$, corresponding to the 3σ interval of the measured value of $\alpha_3^{-1}(M_Z)$. These observations are considered in the third through eighth columns of table 3, where we display the number of vacua with partial and full unification for each choice of Λ_{SUSY} . We realize that, from the huge number of possible effective vacua with \mathcal{G}_{eff} , only a quite small set of \mathbb{Z}_8 orbifold vacua of order hundred in each case satisfies all of our constraints.

In figure 2 we present our results for all \mathbb{Z}_8 orbifold vacua with only $SU(2)_L - U(1)_Y$ unification. The left panels correspond to frequency plots for three different choices of Λ_{SUSY} of (the inverse of) the $U(1)'$ coupling strength α_4^{-1} at the low-energy scale $\Lambda_{Z'} = 2 \text{ TeV}$ against the scale at which $\alpha_1 = \alpha_2$, denoted M_{GUT} . The central values of the largest (red) bubble corresponds to the most frequent combination of $\alpha_4^{-1}(\Lambda_{Z'})$ and M_{GUT} . The small (purple) bubbles correspond to at most six vacua with the combination of values at their center. The right panels are also frequency plots of the values of α_{GUT}^{-1} and M_{GUT} achieved by our vacua, where $\alpha_{GUT} \equiv \alpha_1(M_{GUT}) = \alpha_2(M_{GUT})$. In these plots, small purple bubbles correspond to up to 50 models with the central value of the circles.

Since this is only an intermediate result, we content ourselves with some semi-qualitative remarks. The first observation is that, independently of whether SUSY is broken at low, intermediate or high energies, \mathbb{Z}_8 orbifold vacua with MSSM-like properties do not allow any

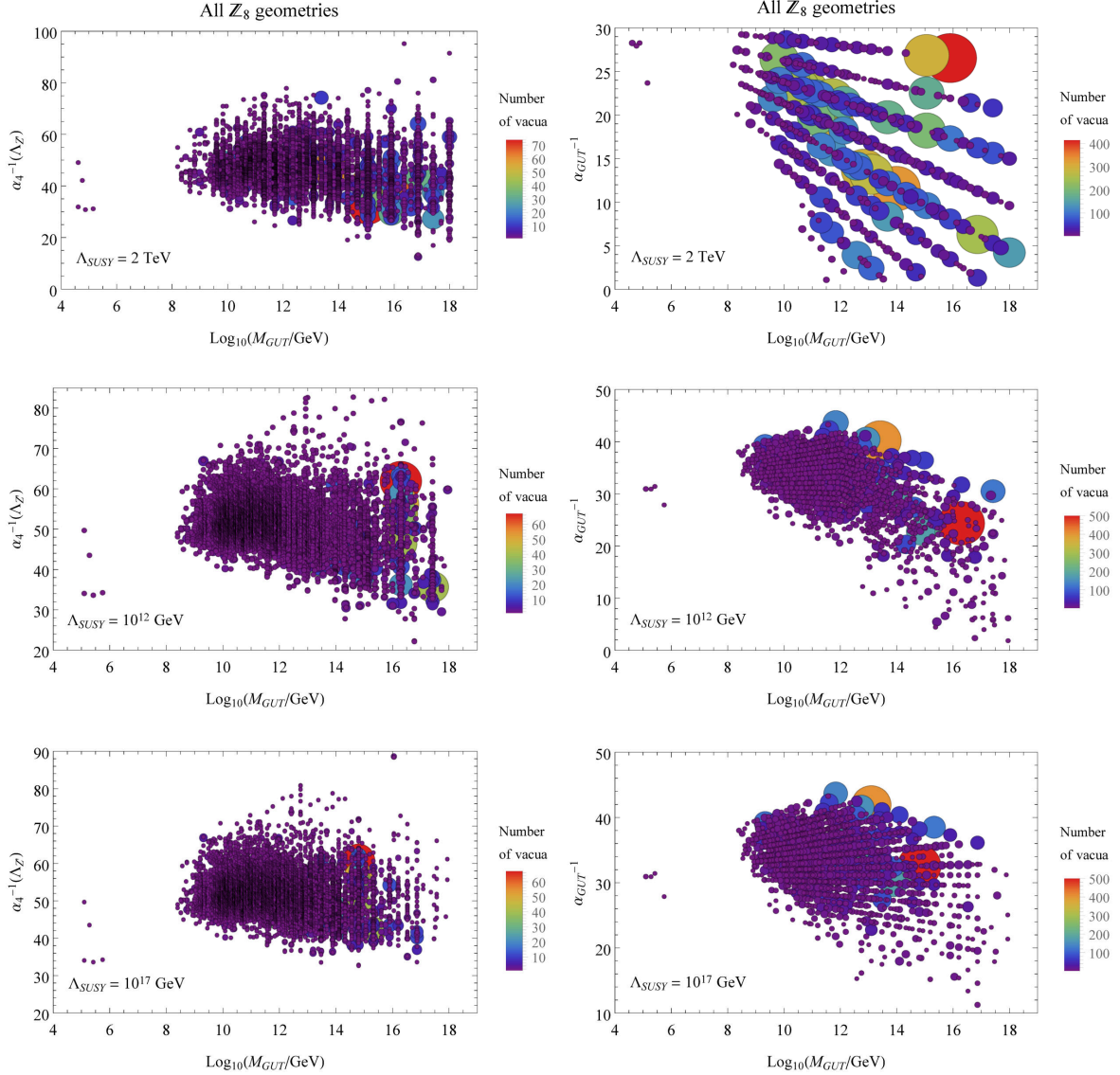


Figure 2: Vacua with different values of M_{GUT} , $\alpha_4^{-1}(\Lambda_{Z'})$ and α_{GUT}^{-1} for three choices of Λ_{SUSY} and partial unification, $\alpha_{GUT} \equiv \alpha_1 = \alpha_2 \neq \alpha_3$. In the left panels, the bubbles in different colors and sizes indicate the number of vacua with the given values of $\alpha_4(\Lambda_{Z'})$ and M_{GUT} at their center. Analogously, the right panels count vacua with different values of α_{GUT} and M_{GUT} .

arbitrary values of $U(1)'$ couplings constants or unification scale. We find that roughly only $20 < \alpha_4^{-1}(2 \text{ TeV}) < 80$, corresponding to $0.4 < g_4(2 \text{ TeV}) < 0.8$, is allowed in our string constructions. We expect this to hold for any heterotic orbifold model with semi-realistic properties. The most common value of $\alpha_4^{-1}(2 \text{ TeV})$ depends on Λ_{SUSY} : for low-scale SUSY $\alpha_4^{-1} \sim 30$, whereas $\alpha_4^{-1} \sim 60$ for other cases. We observe also other rough limits: $M_{GUT} > 10^8 \text{ GeV}$, and $\alpha_{GUT}^{-1} < 30$ for low-scale SUSY and $\alpha_{GUT}^{-1} < 45$ for other SUSY scales.

On the other hand, taking averages over all models, we find $\overline{M_{GUT}} \approx 10^{16} \text{ GeV}$ and $\overline{\alpha_{GUT}^{-1}} \approx 13$ for low-scale SUSY, and $\overline{M_{GUT}} \approx 10^{15} \text{ GeV}$ and $\overline{\alpha_{GUT}^{-1}} \approx 30$ otherwise. Unfortunately, most of these vacua are far from our ideal scenario, with full unification, which can also be measured

by the average difference of $\Delta \equiv |\alpha_{GUT} - \alpha_3(M_{GUT})|$, which is as large as $\bar{\Delta} \approx \alpha_{GUT}$ for low-scale SUSY, and $\bar{\Delta} \approx \frac{1}{3}\alpha_{GUT}$ for higher Λ_{SUSY} .

Let us comment on the vertical (diagonal) alignment pattern of the points in the left (right) plots of figure 2. Consider e.g. the top plots, with $\Lambda_{SUSY} = \Lambda_{Z'}$, where one can find that the RGE lead to

$$\ln \frac{M_{GUT}}{\Lambda_{Z'}} = 2\pi (\alpha_1^{-1}(\Lambda_{Z'}) - \alpha_2^{-1}(\Lambda_{Z'})) \frac{1}{b_1 - b_2}.$$

Since only M_{GUT} and $b_1 - b_2$ are model-dependent, all vacua with the same difference $b_1 - b_2$ lead to the same M_{GUT} , yielding a point on the same vertical line in the left panels of the figure. Further, as not any arbitrary b_i can appear in our vacua (but only rational numbers), this difference does not build a continuous, producing separate lines. The origin of the diagonal lines in the right panels is simpler. The RGE lead to $\alpha_{GUT}^{-1} = \alpha_2^{-1}(M_{GUT}) = \alpha_2^{-1}(\Lambda_{Z'}) - \frac{b_2}{2\pi} \ln \frac{M_{GUT}}{\Lambda_{Z'}}$, as a result of the running of α_2 ; each diagonal line describes this running for a given b_2 , populated by all vacua with the same b_2 .

In figure 3 we present our main results: the values of $\alpha_4(\Lambda_{Z'})$, α_{GUT} and M_{GUT} in the \mathbb{Z}_8 orbifold vacua with gauge coupling unification. As before, we present how often we find in our effective vacua the few admissible values of the $U(1)'$ coupling strength at reachable energies, $\alpha_4(\Lambda_{Z'})$, the scale at which all coupling strengths meet, M_{GUT} , and the value of the coupling strengths when they meet, $\alpha_{GUT} = \alpha_i(M_{GUT})$, $i = 1, 2, 3$. From the top to the bottom plots, we display these results for the SUSY scales, $\Lambda_{SUSY} = 2 \text{ TeV}$, 10^{12} GeV and 10^{17} GeV .

For low-SUSY scale, we observe that the $U(1)'$ coupling strength is quite restricted by $25 \leq \alpha_4^{-1}(2 \text{ TeV}) \leq 60$, or equivalently $0.46 \leq g_4(2 \text{ TeV}) \leq 0.7$; the only allowed unification scales are $M_{GUT} \in \{10^{12} \text{ GeV}, 6.6 \times 10^{13} \text{ GeV}, 4.1 \times 10^{16} \text{ GeV}\}$; and the coupling at unification takes only a few values, restricted by $5.6 \leq \alpha_{GUT}^{-1} \leq 21.4$. We note that $g_4(2 \text{ TeV}) \approx 0.6$ is the most commonly present value, just below the observed value of the $SU(2)_L$ coupling. Additionally, most of the vacua (62 out of 77) find unification at the largest M_{GUT} . At that scale, the preferred value of the GUT coupling corresponds to $\alpha_{GUT} \approx 1/21$, very close to the value taken traditionally in GUTs, $\alpha_{GUT} \approx 1/25$. As a side remark, although we have considered $\alpha_i = 1$ as our perturbativity limit, a stricter bound is achieved if one demands $g_i < 1$, which would imply that the values $\alpha_{GUT}^{-1} \lesssim 11$ should be disregarded and, in turn, so should the vacua with the lowest GUT scale $M_{GUT} = 10^{12} \text{ GeV}$ in this case.

For intermediate scale SUSY breaking, the variety of \mathbb{Z}_8 orbifold vacua with unification is richer. However, once more, there are strong restrictions on the possibly observable values of the $U(1)'$ couplings, set by $38 < \alpha_4^{-1}(2 \text{ TeV}) \leq 64$, or equivalently $0.44 \leq g_4(2 \text{ TeV}) < 0.6$. Since the distribution of $U(1)'$ coupling values at low energies is quite uniform, its average value can also be of some interest: $\overline{g_4(2 \text{ TeV})} \approx 0.5$. Concerning the unification scale and the coupling at those energies, we find a very compact distribution of values with $4.3 \times 10^{11} \text{ GeV} \leq M_{GUT} \leq 10^{16} \text{ GeV}$ and $17 < \alpha_{GUT}^{-1} < 36$. Most of the vacua yield $M_{GUT} \approx 4.3 \times 10^{11} \text{ GeV}$ and $\alpha_{GUT} \approx 1/33$. It is interesting that the higher the SUSY breaking scale, the lower the unification scale.

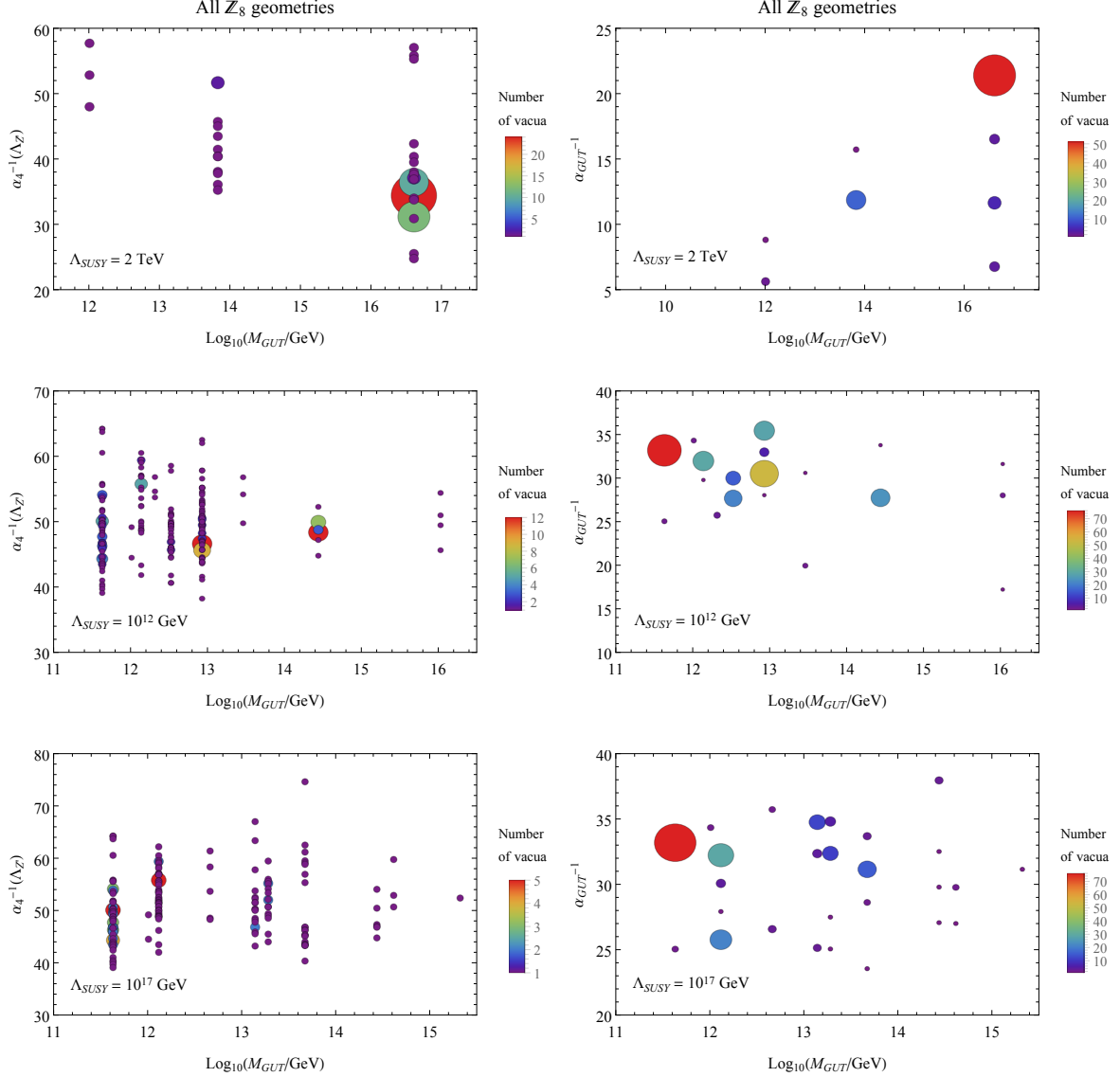


Figure 3: Vacua with different values of M_{GUT} , $\alpha_4^{-1}(\Lambda_{Z'})$ and α_{GUT}^{-1} for three choices of Λ_{SUSY} and partial unification, $\alpha_{GUT} \equiv \alpha_1 = \alpha_2 \approx \alpha_3$. In the left panels, the bubbles in different colors and sizes indicate the number of vacua with the given values of $\alpha_4(\Lambda_{Z'})$ and M_{GUT} at their center. Analogously, the right panels count vacua with different values of α_{GUT} and M_{GUT} .

An intriguing observation is that models without SUSY below M_{str} emerging from heterotic orbifold compactifications produce very similar results (roughly identical in our approximations) to those of intermediate SUSY scale. In particular, inspecting the bottom-left panel, we see that the range of values for $\alpha_4^{-1}(2 \text{ TeV})$ coincides with the previous case, except for an isolated vacuum, which we might ignore. As a consequence, again, $\overline{g_4} \approx 0.5$ at low energies. In fact, most of the vacua of this type render *exactly* the same M_{GUT} and α_{GUT} as in the previous case.

5 Sample model with potentially stable Higgs vacuum

To illustrate the features of our promising vacua with $U(1)'$, let us examine in one \mathbb{Z}_8 orbifold sample vacuum the potential of a $U(1)'$ as a tool to solve the metastability problem of the Higgs potential. According to ref. [6], SM fermions and some extra singlets with $U(1)'$ charges, subject to a series of constraints, can ameliorate the RGE running of the relevant couplings, yielding a positive Higgs self-coupling at all scales.

The shift vector V and WL W_a (satisfying the constraints in table 1) that define the gauge embedding of a particular \mathbb{Z}_8 -II (2,1) orbifold are

$$\begin{aligned} V &= \frac{1}{4}(-7/2, 0, 0, 0, 1/2, 1/2, 5/2, 3)(-4, -1, 0, 0, 0, 1/2, 1/2, 3), \\ W_1 &= \frac{1}{4}(1, -7, -7, -5, 2, 2, 1, -3)(-3, 3, -6, -4, 1, -3, 3, 5), \quad W_6 = 0. \end{aligned} \quad (9)$$

The resulting gauge group $\mathcal{G}_{4D} = \mathcal{G}_{SM} \times [U(1)']^6 \times SU(2)^6$, where one $U(1)'$ is (pseudo-)anomalous. We choose a vacuum of SM singlet VEVs, such that $\mathcal{G}_{4D} \rightarrow \mathcal{G}_{\text{eff}}$ (see eq. (4)) spontaneously and the (correctly normalized) hypercharge and $U(1)'$ generators are given by

$$\begin{aligned} t_1 &= \frac{1}{4}(-1, -5/3, -5/3, 5/3, -1, -1, 1, 1)(0, 0, 0, 0, 0, 0, 0, 0), \\ t_4 &= \frac{1}{12\sqrt{2}}(-3, 0, 0, 0, 1, 1, 1, -2)(0, 0, 0, 0, 0, 8, 8, 0). \end{aligned} \quad (10)$$

The spectrum of the chosen vacuum, after the decoupling of exotics w.r.t. \mathcal{G}_{eff} , is displayed in table 4, considering scales below $\Lambda_{SUSY} = 10^{12}$ GeV. It contains the SM particles, an extra Higgs boson, few fermionic exotics and some SM singlets, which are mostly fermions. We choose as scalars two (instead of one) SM singlets, s_1 and s_2 , to trigger the spontaneous breakdown of $U(1)'$ and facilitate the decoupling of SM exotics.

We compute the RGE running of the couplings with $b_i \in \{59/5, 5, -2, 731/72\}$ below Λ_{SUSY} , as shown in fig. 4. We find that $g_4(2 \text{ TeV}) \approx 0.48$. With this value and supposing that H_u dominates the quartic Higgs self-coupling, we expect that the analysis of ref. [6] can be applied. Following their discussion, we notice that, in order to diagnose whether the Higgs metastability is alleviated in our vacuum, we must consider the $U(1)'$ charges of a few SM particles, and compare with the stable regions of figure 1 in that reference. In their notation, the $U(1)'$ charges to consider are $Q_{q_3} = q_{q_3} = 1/4\sqrt{2}$, $Q_h = q_{H_u} = -1/3\sqrt{2}$ and $Q_4 = \sqrt{b_4} \approx 2.43$. Unfortunately, in ref. [6], only $g_4 \leq 0.3$ is explored, but, extrapolating their results, it is possible to expect that our charges and $U(1)'$ coupling constant combine together to lie in a region with a stable Higgs vacuum for a multi-TeV Z' .

This model admits further interesting phenomenology. E.g. we find that, at this level, the Yukawa coupling of the third generation, $q_3 \bar{u}_3 H_u$, is the largest, as expected, because it is renormalizable. Other Yukawas, such as $q_{1,2} \bar{u}_{1,2} H_u$, appear as soon as the $U(1)'$ is broken spontaneously. Very schematically, the dominant contributions to the mass terms are given by

$$\begin{aligned} & q_3 \bar{u}_3 H_u + q_{1,2} \bar{u}_{1,2} H_u s_2^2 + q_3 \bar{d}_3 H_d s_1^7 s_2^2 + q_{1,2} \bar{d}_{1,2} H_d s_2^2 \\ & + \ell_3 \bar{e}_3 H_d s_1^2 + \ell_{1,2} \bar{e}_{1,2} H_d s_2^2 + \ell_3 N_i^b H_u s_2^2 + N_i^a N_j^c s_1, \end{aligned}$$

#	Fermionic irrep	Label	#	Fermionic irrep	Label	#	Scalar irrep	Label
2	(1, 2) _(1/2, -7/12√2)	$\ell_{1,2}$	1	(3, 1) _(-1/3, 3/4√2)	\bar{x}_i	1	(1, 2) _(-1/2, -1/3√2)	H_u
1	(1, 2) _(1/2, 1/3√2)	ℓ_3	1	(3, 1) _(1/3, 1/12√2)	x_i	1	(1, 2) _(1/2, 1/12√2)	H_d
2	(1, 1) _(-1, -1/6√2)	$\bar{e}_{1,2}$	8	(1, 2) _(0, 1/6√2)	η_i	1	(1, 1) _(0, -1/4√2)	s_1
1	(1, 1) _(-1, 1/12√2)	\bar{e}_3	8	(1, 1) _(-1/2, 1/6√2)	ζ_i	1	(1, 1) _(0, 1/3√2)	s_2
2	(3, 2) _(-1/6, -1/6√2)	$q_{1,2}$	8	(1, 1) _(1/2, 7/12√2)	$\bar{\zeta}_i$			
1	(3, 2) _(-1/6, 1/4√2)	q_3	8	(1, 1) _(1/2, -1/12√2)	$\bar{\kappa}_i$			
2	(3, 1) _(2/3, -1/6√2)	$\bar{u}_{1,2}$	8	(1, 1) _(-1/2, -1/6√2)	κ_i			
1	(3, 1) _(2/3, 1/12√2)	\bar{u}_3	11	(1, 1) _(0, 1/3√2)	N_i^a			
2	(3, 1) _(-1/3, -7/12√2)	$\bar{d}_{1,2}$	10	(1, 1) _(0, -2/3√2)	N_i^b			
1	(3, 1) _(-1/3, 3/4√2)	\bar{d}_3	8	(1, 1) _(0, -1/12√2)	N_i^c			
			6	(1, 1) _(0, -5/12√2)	N_i^d			
			4	(1, 1) _(0, 7/12√2)	N_i^e			
			2	(1, 1) _(0, -1/4√2)	N_i^f			

Table 4: Massless spectrum for a vacuum with gauge group \mathcal{G}_{eff} . Representations with respect to $\text{SU}(3)_c \times \text{SU}(2)_L$ are given in bold face, the hypercharge and the $\text{U}(1)'$ charge are indicated as subscript. The frame on the left corresponds to the SM fermions, the middle frame to fermionic exotics, and the right frame shows scalars including the Higgs fields.

where the singlet VEVs can be chosen, so that some fine-tuning $\langle s_1 \rangle \gg \langle s_2 \rangle$ and $\langle s_1 \rangle > \Lambda_{Z'} > \langle s_2 \rangle$ could be allowed, to furnish quarks and charged leptons with approximately right mass hierarchies. We observe that there is also the possibility of obtaining masses for the neutrinos N_i through a type-I see-saw mechanism. The exotics of the middle frame of table 4 can also develop masses while $\text{U}(1)'$ breaks, although their masses would be of order $\Lambda_{Z'}$ and should be soon detected. The precise analysis of all this phenomenology is beyond the scope of this letter. We content ourselves here with sketching the phenomenological potential of this model and leave the details for future work.

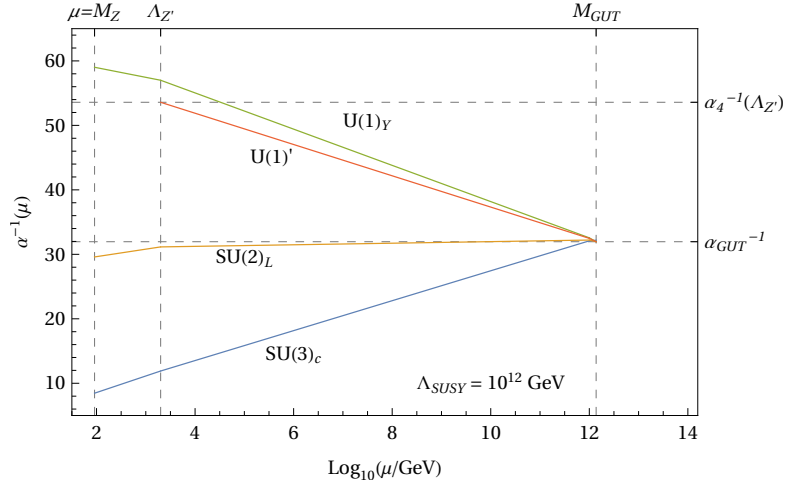


Figure 4: RGE running of the gauge coupling strengths of $\text{U}(1)_Y$, $\text{SU}(2)_L$, $\text{SU}(3)_C$ and $\text{U}(1)'$ in a \mathbb{Z}_8 -II (2,1) sample vacuum. They meet at $M_{GUT} \approx 1.4 \times 10^{12}$ GeV with a value $\alpha_{GUT} \approx 1/32$. From this plot, one can read off that, at $\Lambda_{Z'} = 2$ TeV, the $\text{U}(1)'$ coupling has the value $g_4 \approx 0.48$.

6 Final remarks and outlook

By means of the 1-loop RGE, we have systematically studied the TeV-scale value of the $U(1)'$ coupling constant in vacua arising from \mathbb{Z}_8 heterotic orbifold compactifications whose matter content exhibits the MSSM spectrum plus vectorlike exotics at the string scale. We have restricted ourselves to vacua with only one non-anomalous $U(1)'$ gauge symmetry, and whose SM gauge couplings have the observed values and unify at a model-dependent GUT scale, below the string scale. Only between 0.5% and 1.5% of all possible vacua satisfy these conditions.

Supposing that the $U(1)'$ breakdown scale is of order of few TeV, reachable at colliders, we find that for TeV SUSY the $U(1)'$ coupling constant is restricted in our constructions to lie in the small range $0.46 < g_4 < 0.7$. This range is further reduced to $0.44 < g_4 < 0.6$ if one allows SUSY to be broken at a scale larger than 10^{12} GeV. Models with such couplings exhibit exotic fermions, in addition to a multi-TeV Z' , that may be detected soon.

We have found that also the unification scale is restricted in \mathbb{Z}_8 orbifold vacua to be roughly either 10^{14} GeV or 10^{16} GeV for low-scale SUSY, or preferably about 10^{12} GeV for intermediate SUSY breaking scale or higher.

We have also studied the properties of a sample model, finding that, if intermediate scale SUSY is realized, there are \mathbb{Z}_8 orbifold vacua that may be furnished with the ingredients to stabilize the Higgs vacuum. The details of such vacua and mechanism are left for future work.

In our scheme, the dynamics of the spontaneous breaking of $U(1)'$ requires large fine-tuning to establish the hierarchies $\Lambda_{Z'} \ll \Lambda_{SUSY} \ll M_{str}$. In a model-dependent basis, it could however be possible that the potential of SM singlets and gaugino condensates conspire to yield such hierarchies. One may also wonder whether this simplifies in non-supersymmetric heterotic orbifolds. Another issue is the details of the RGE at the SUSY breaking scale, including the decoupling of superpartners, which may require a treatment such as in [55]. These important questions shall be the goal of future projects.

Acknowledgments. It is a pleasure to thank Jens Erler for very useful discussions and motivation to pursue this work. SR-S would like to thank Rafael Alapisco-Arambula, who participated in an early stage of this project. SR-S is grateful to the Bethe Center for Theoretical Physics and the Mainz Institute for Theoretical Physics for the hospitality. This work was partly supported by DGAPA-PAPIIT grant IN100217 and CONACyT grants F-252167 and 278017.

References

- [1] P. Langacker, Rev. Mod. Phys. **81** (2009), 1199, [arXiv:0801.1345](#) [hep-ph].
- [2] O. Lebedev and Y. Mambrini, Phys. Lett. **B734** (2014), 350, [arXiv:1403.4837](#) [hep-ph].

- [3] J. G. Rodrigues, A. C. O. Santos, J. G. Ferreira, and C. A. de S. Pires, [arXiv:1807.02204](#) [hep-ph].
- [4] J. Ellis, M. Fairbairn, and P. Tunney, [arXiv:1807.02503](#) [hep-ph].
- [5] W. Altmannshofer, C.-Y. Chen, P. S. Bhupal Dev, and A. Soni, Phys. Lett. **B762** (2016), 389, [arXiv:1607.06832](#) [hep-ph].
- [6] S. Di Chiara, V. Keus, and O. Lebedev, Phys. Lett. **B744** (2015), 59, [arXiv:1412.7036](#) [hep-ph].
- [7] R. Martinez, F. Ochoa, and J. P. Rubio, Phys. Rev. **D89** (2014), no. 5, 056008, [arXiv:1303.2734](#) [hep-ph].
- [8] A. Celis, J. Fuentes-Martin, M. Jung, and H. Serodio, Phys. Rev. **D92** (2015), no. 1, 015007, [arXiv:1505.03079](#) [hep-ph].
- [9] J. S. Kim, O. Lebedev, and D. Schmeier, JHEP **11** (2015), 128, [arXiv:1507.08673](#) [hep-ph].
- [10] J. Erler, Nucl. Phys. **B586** (2000), 73, [arXiv:hep-ph/0006051](#) [hep-ph].
- [11] D. A. Demir, G. L. Kane, and T. T. Wang, Phys. Rev. **D72** (2005), 015012, [arXiv:hep-ph/0503290](#) [hep-ph].
- [12] ATLAS, M. Aaboud et al., JHEP **10** (2017), 182, [arXiv:1707.02424](#) [hep-ex].
- [13] ATLAS, M. Aaboud et al., JHEP **01** (2018), 055, [arXiv:1709.07242](#) [hep-ex].
- [14] ATLAS, M. Aaboud et al., Eur. Phys. J. **C78** (2018), no. 7, 565, [arXiv:1804.10823](#) [hep-ex].
- [15] ATLAS, M. Aaboud et al., Phys. Rev. **D98** (2018), 032016, [arXiv:1805.09299](#) [hep-ex].
- [16] J. Erler, P. Langacker, S. Munir, and E. Rojas, JHEP **11** (2011), 076, [arXiv:1103.2659](#) [hep-ph].
- [17] J. Erler, P. Langacker, S. Munir, and E. Rojas, *Z' Bosons from E(6): Collider and Electroweak Constraints*, in *19th International Workshop on Deep-Inelastic Scattering and Related Subjects (DIS 2011) Newport News, Virginia, April 11-15, 2011*, 2011.
- [18] E. Rojas and J. Erler, JHEP **10** (2015), 063, [arXiv:1505.03208](#) [hep-ph].
- [19] R. H. Benavides, L. Muñoz, W. A. Ponce, O. Rodríguez, and E. Rojas, Int. J. Mod. Phys. **A33** (2018), no. 35, 1850206, [arXiv:1801.10595](#) [hep-ph].
- [20] M. Cvetič, J. Halverson, and P. Langacker, JHEP **11** (2011), 058, [arXiv:1108.5187](#) [hep-ph].

- [21] G. B. Cleaver and A. E. Faraggi, Int. J. Mod. Phys. **A14** (1999), 2335, [arXiv:hep-ph/9711339](#) [hep-ph].
- [22] C. Coriano, A. E. Faraggi, and M. Guzzi, Eur. Phys. J. **C53** (2008), 421, [arXiv:0704.1256](#) [hep-ph].
- [23] J. Halverson and P. Langacker, *Remnants from the String Landscape*, in *Theoretical Advanced Study Institute in Elementary Particle Physics: Physics at the Fundamental Frontier (TASI 2017) Boulder, CO, USA, June 5-30, 2017*, 2018.
- [24] P. Athanasopoulos, A. E. Faraggi, and V. M. Mehta, Phys. Rev. **D89** (2014), no. 10, 105023, [arXiv:1401.7153](#) [hep-th].
- [25] A. E. Faraggi and J. Rizos, Nucl. Phys. **B895** (2015), 233, [arXiv:1412.6432](#) [hep-th].
- [26] W. Buchmüller, K. Hamaguchi, O. Lebedev, and M. Ratz, Nucl. Phys. **B785** (2007), 149, [hep-th/0606187](#).
- [27] O. Lebedev, H. P. Nilles, S. Raby, S. Ramos-Sánchez, M. Ratz, P. K. S. Vaudrevange, and A. Wingerter, Phys. Rev. **D77** (2007), 046013, [arXiv:0708.2691](#) [hep-th].
- [28] H. M. Lee, S. Raby, M. Ratz, G. G. Ross, R. Schieren, K. Schmidt-Hoberg, and P. K. Vaudrevange, Nucl. Phys. **B850** (2011), 1, [arXiv:1102.3595](#) [hep-ph].
- [29] S. Groot Nibbelink and O. Loukas, JHEP **12** (2013), 044, [arXiv:1308.5145](#) [hep-th].
- [30] M. Goodsell, S. Ramos-Sánchez, and A. Ringwald, JHEP **01** (2012), 021, [arXiv:1110.6901](#) [hep-th].
- [31] Y. Olguín-Trejo, R. Pérez-Martínez, and S. Ramos-Sánchez, Phys. Rev. **D98** (2018), no. 10, 106020, [arXiv:1808.06622](#) [hep-th].
- [32] M. Fischer, M. Ratz, J. Torrado, and P. K. S. Vaudrevange, JHEP **1301** (2013), 084, [arXiv:1209.3906](#) [hep-th].
- [33] F. Plöger, S. Ramos-Sánchez, M. Ratz, and P. K. S. Vaudrevange, JHEP **04** (2007), 063, [arXiv:hep-th/0702176](#) [hep-th].
- [34] S. Ramos-Sánchez and P. K. S. Vaudrevange, JHEP **01** (2019), 055, [arXiv:1811.00580](#) [hep-th].
- [35] L. J. Dixon, J. A. Harvey, C. Vafa, and E. Witten, Nucl. Phys. **B261** (1985), 678.
- [36] L. J. Dixon, J. A. Harvey, C. Vafa, and E. Witten, Nucl. Phys. **B274** (1986), 285.
- [37] S. Ramos-Sánchez, Fortsch. Phys. **10** (2009), 907, [arXiv:0812.3560](#) [hep-th].
- [38] P. K. S. Vaudrevange, *Grand Unification in the Heterotic Brane World*, Ph.D. thesis, Bonn U., 2008.

- [39] H. P. Nilles, S. Ramos-Sánchez, P. K. S. Vaudrevange, and A. Wingerter, *Comput.Phys.Commun.* **183** (2012), 1363, [arXiv:1110.5229 \[hep-th\]](#), web page <http://projects.hepforge.org/orbifolder/>.
- [40] Y. Olguín-Trejo, R. Pérez-Martínez, and S. Ramos-Sánchez, *Tables of Abelian heterotic orbifolds and their flavor symmetries*, 2018, <http://stringpheno.fisica.unam.mx/stringflavor/>.
- [41] E. Witten, *Phys. Lett.* **B149** (1984), 351.
- [42] M. B. Green and J. H. Schwarz, *Phys. Lett.* **B149** (1984), 117.
- [43] O. Lebedev, H. P. Nilles, S. Raby, S. Ramos-Sánchez, M. Ratz, P. K. S. Vaudrevange, and A. Wingerter, *Phys. Lett.* **B645** (2007), 88, [hep-th/0611095](#).
- [44] O. Lebedev, H. P. Nilles, S. Ramos-Sánchez, M. Ratz, and P. K. S. Vaudrevange, *Phys. Lett.* **B668** (2008), 331, [arXiv:0807.4384 \[hep-th\]](#).
- [45] S. L. Parameswaran, S. Ramos-Sánchez, and I. Zavala, *JHEP* **1101** (2011), 071, [arXiv:1009.3931 \[hep-th\]](#).
- [46] B. Dundee, S. Raby, and A. Westphal, *Phys.Rev.* **D82** (2010), 126002, [arXiv:1002.1081 \[hep-th\]](#).
- [47] Particle Data Group, C. Patrignani et al., *Chin. Phys.* **C40** (2016), no. 10, 100001 and 2017 update.
- [48] CMS, A. M. Sirunyan et al., Submitted to: *JHEP* (2018), [arXiv:1812.06302 \[hep-ex\]](#).
- [49] ATLAS, M. Aaboud et al., Submitted to: *Phys. Rev.* (2018), [arXiv:1812.09432 \[hep-ex\]](#).
- [50] L. E. Ibáñez and I. Valenzuela, *JHEP* **05** (2013), 064, [arXiv:1301.5167 \[hep-ph\]](#).
- [51] M. Blaszczyk, S. Groot-Nibbelink, O. Loukas, and S. Ramos-Sánchez, *JHEP* **10** (2014), 119, [arXiv:1407.6362 \[hep-th\]](#).
- [52] S. Groot Nibbelink, O. Loukas, and F. Ruehle, *Fortsch. Phys.* **63** (2015), 609, [arXiv:1507.07559 \[hep-th\]](#).
- [53] S. Abel, E. Dudas, D. Lewis, and H. Partouche, [arXiv:1812.09714 \[hep-th\]](#).
- [54] O. Lebedev, H. P. Nilles, S. Raby, S. Ramos-Sánchez, M. Ratz, P. K. S. Vaudrevange, and A. Wingerter, *Phys. Rev. Lett.* **98** (2007), 181602, [hep-th/0611203](#).
- [55] M. Beneke, P. Ruiz-Femenia, and M. Spinrath, *JHEP* **01** (2009), 031, [arXiv:0810.3768 \[hep-ph\]](#).